

Evaluation of acrylate penetration into printing blanket by IR imaging

Yasushi Ozaki*, Asuka Uchida*

Keywords: UV, Cure, Ink, Acrylate, IR, Imaging, Blanket

Abstract

In order to illuminate the penetration of UV curable ink vehicle into press blanket, IR imaging system was used as a new technique. Cross sections of blanket were prepared for IR imaging. Spectra data for imaging were collected by moving the sample stage automatically. Acrylate and UV curable ink into blanket could be characterized as a single wave-number map. In addition, each component in the UV curable ink could be characterized with a Principal Component Analysis (PCA).

The penetration rate of low-viscosity acrylate was the same as that of UV curable ink with high viscosity. Moreover, the penetration rate of vehicle into the blanket was in order of acrylate monomer > acrylate oligomer > pre-polymer. This meant that the penetration of the acrylate monomer was affected that of UV curable ink into blanket. In addition, the photo initiator transferred together with acrylate monomer in the blanket.

Introduction

In recent years, UV curable inks have become popular in offset printing due to their solvent free nature (Stowe, 2004). Some acrylates are used as the vehicle of UV curable ink. The interaction of printing press blankets with acrylates can influence the printing results and integrity of the blanket because acrylates will penetrate into the blanket for printing. It is important to investigate the behavior of acrylates in blankets. However, little has been reported on the penetration rate of acrylate into commercial blankets. Especially, we have not yet seen a study considering the penetration of photo initiator in blankets. We have studied about the penetration of solvents into press blankets by confocal laser scanning microscope (CLSM) (Ozaki, 2007). Although a simple component such as a solvent can be observed using CLSM, mixtures such as ink vehicles cannot be evaluated by this technique.

*:Research Institute, National Printing Bureau of Japan

In order to illuminate the behavior of UV curable ink vehicle, IR imaging system was used as a new technique. IR imaging system was developed from mapping analysis for microscope IR spectroscopy and was improved as a high speed imaging instrument. 16 spectra were obtained simultaneously in IR imaging system because 16 detectors formed a line. Spectra data for the imaging was collected by moving the sample stage automatically. Characteristic peak at a single wave-number, for example the C-H stretching vibration at 2930cm^{-1} or the C=O stretching vibration at 1720cm^{-1} , can be selected for chemical map.

In the case of components having similar IR spectra, it is difficult to discriminate similar components from characteristic peak. Principal Component Analysis (PCA) has been applied to simplify the data analysis and improve chemical contrast. PCA is a statistical method used to find the combination of the variables that describe the most important trends in the data (Green,1988, Lee,1990). PCA was often used to simplify complicated IR spectra (Marengo,2005,Pereira,2006,Elliott,2007). PCA has also proven valuable in analyzing and improving contrast in the time of flight - secondary ion mass spectrometry (TOF-SIMS) images (Vanden,1997, Sun,2004).

In this study, the penetration of acrylate into printing press blankets using an IR imaging system is reported. Acrylate and UV curable ink into blanket are characterized as single wave-number map. In addition, each component in UV curable ink vehicle is characterized as PCA map.

Experimental

An UV curable ink type blanket that was produced by Sumitomo Rubber Co. was used. The rubber had been stuck on the reinforcement cloth. The rubber of blanket was mainly determined to be isoprene rubber, and aluminum oxide and silica were included as fillers in the rubber. The thickness of the blanket rubber was about $350\mu\text{m}$.

Acrylate-A (MANDA (acrylate monomer): Japan Chem. Co.) as diluent and UV curable magenta ink (Septer DX, DIC Co.) were prepared for the acrylate penetration test. The viscosities of acrylate-A and UV curable ink were 0.09Pa s and 60.24Pa s , respectively. In addition, typical UV curable ink vehicle was also prepared to confirm how each constituent in ink vehicle would penetrate into the blanket. This vehicle composition was indicated in Table.1.

Table 1 Vehicle Composition

Monomer (Dipentaerythritol Hexaacrylate)	40%
Oligomer (Urethane Acrylate)	30%
Pre-polymer (Diallyl Telephthalate Prepolymer)	20%
Photo initiator (-Amino Acetophenone)	10%

To prepare samples for IR imaging, the following procedure was performed: (1) Each acrylate was applied at a constant volume (40 μ l) on the blanket (area :1cm²). (2) Excess acrylate was wiped off after several hours. (3) The blanket was cut from the rear by a delicate cutter (JUSCO Co.) in order to prevent acrylate from running with the cutting edge. (4) Finally, the cross sections of the blanket were prepared as samples for IR imaging.

IR imaging was carried out by IR imaging system (Spotlight-300: Perkin Elmer Co.). The cross section of each sample was set on the sample stage of IR microscope. The reflection mode was used to measure samples. The measurement area was adjusted to 700 μ m x 2000 μ m. 35840 spectra were obtained in this area because IR beam size was 6.25 μ m x 6.25 μ m. It only took about 20 minutes to measure one sample through high speed detection system. Spectral range was from 4000cm⁻¹ to 720cm⁻¹ at 8cm⁻¹ spectral resolution. All reflection spectra for IR imaging were transferred to absorbance, after Kramers-Krönig (K-K) transformation was executed. The strain of reflection spectra can be revised by K-K transformation.

Results and Discussion

Penetration of acrylate into blanket

The IR spectra of blanket rubber, acrylate -A and UV curable ink were shown in Figure 1. The strong peak of carbonyl group (C=O) at 1735cm⁻¹ was detected from acrylate -A and UV curable ink. UV curable ink also had C=O band depending on the acrylate. However, blanket rubber had no peak at this wave-number. As a result, the acrylate could be distinguish from the blanket rubber using the C=O band at 1735cm⁻¹ on IR imaging system.

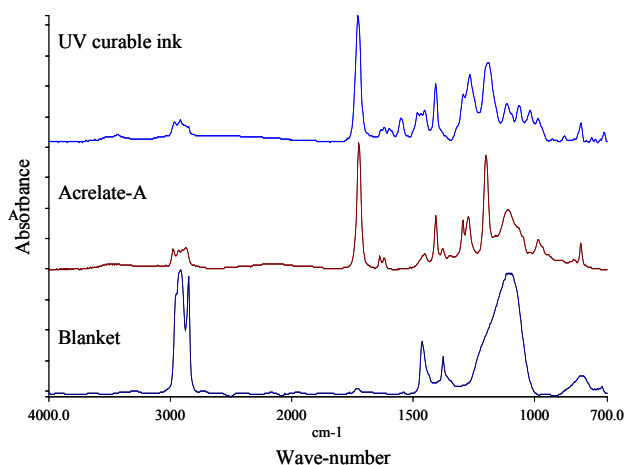


Figure 1 IR spectra of blanket rubber, acrylate-A and UV curable ink

Figure 2 shows the optical microscope image of a blanket cross section (top) and imaging IR maps in the red frame area on the upper image 30 minutes after acrylate-A was dropped on the blanket. The total absorbance map and the single frequency map at 1735cm^{-1} were shown on the bottom. The intensity of absorbance on each point was represented by a color bar. The configuration of the cross section of the blanket could be found by the total absorbance map. That acrylate-A had penetrated into the blanket rubber could be visualized by the single frequency map at 1735cm^{-1} .

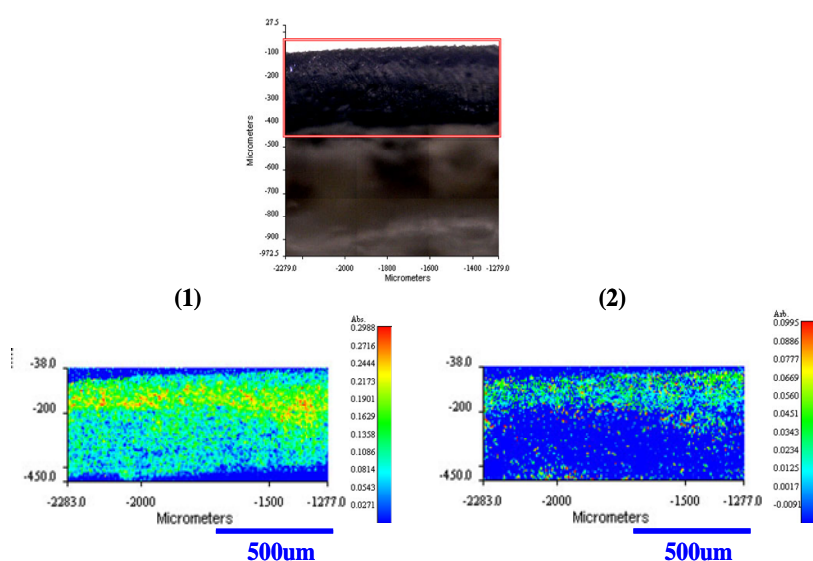


Figure 2 Optical microscope image of blanket cross section (top) and imaging IR maps (bottom) 30 minutes after acrylate-A was dropped on blanket

IR imaging was carried out in the red frame of blanket cross section.

(1) Total absorbance map (2) Single frequency map at 1735cm^{-1}

Figure 3 shows single frequency maps at 1735cm^{-1} ($\text{C}=\text{O}$ stretching vibration) on the cross section of blanket after several hours. The acrylate -A hardly penetrated just after dropping onto the blanket. However, the acrylate -A had already penetrated to the middle of blanket rubber in one hour after dropping. Moreover, the acrylate -A was distributed throughout the entire blanket rubber 24 hours later, and some of acrylate -A arrived at the interface between rubber and the reinforcement cloth 48 hours later.

Figure 4 shows the relationship between the penetration depth and time after acrylate-A dropping. The penetration depth was quantified as the average value

from the distribution of acrylate-A in figure 3. The penetration rate of acrylate into printing blanket could be evaluated from cross sections of blanket using IR imaging system.

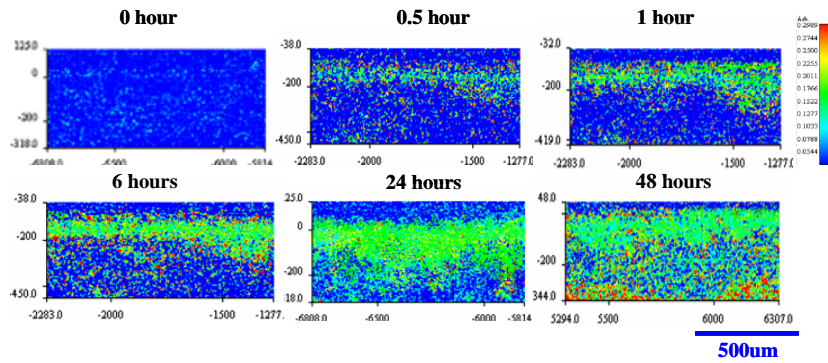


Figure 3 Single frequency maps at 1735cm^{-1} ($\text{C}=\text{O}$ stretching vibration of acrylate-A) on the cross section of blanket after various time periods

Figure 5 shows the relationship between the penetration depth and time after UV curable ink dropping, similar to acrylate-A. Although the viscosity of acrylate-A was much lower than that of UV curable ink, the penetration rate of acrylate-A was almost same as that of UV curable ink. In order to resolve this phenomenon, the penetration rates of acrylate monomer, acrylate oligomer and pre-polymer in blanket were investigated by IR imaging system. In this case, the mixture of acrylate monomer, acrylate oligomer, pre-polymer and photo initiator was used as the UV curable ink vehicle because all components in ink vehicle could be simultaneously characterized into blanket.

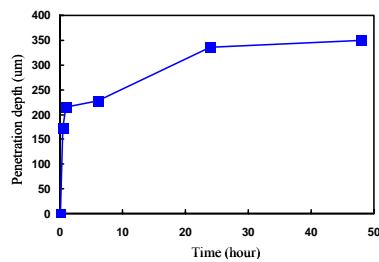


Figure 4 Relationship between penetration depth and time after acrylate-A dropping

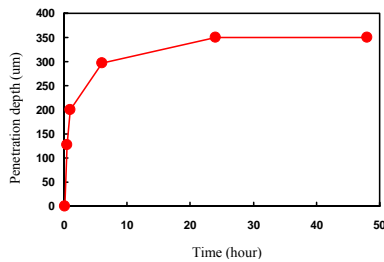


Figure 5 Relationship between penetration depth and time after UV curable ink dropping, similar to acrylate-A

Penetration of UV curable ink vehicle components

Figure 6 shows the IR reflection spectrum (2000 to 700 cm^{-1}) of blanket rubber, reinforcement cloth, acrylate monomer, acrylate oligomer, pre-polymer and photo initiator respectively. The difference of penetration behavior between acrylate monomer, acrylate oligomer and pre-polymer could not be determined from the peak of carbonyl group (C=O) at 1735 cm^{-1} because these components always had a C=O band in their chemical structure. The other peaks could not well represent the difference between acrylate monomer, acrylate oligomer and pre-polymer.

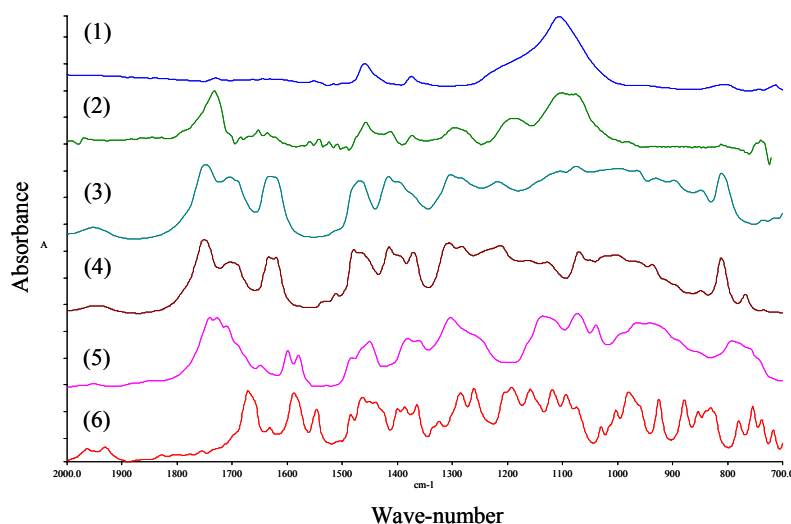


Figure 6 IR reflection spectrum (2000 to 700 cm^{-1}) of (1)blanket rubber,(2)reinforcement cloth, (3)acrylate monomer, (4)acrylate oligomer, (5) pre-polymer and (6)photo initiator

Eventually, Principal Component Analysis (PCA) referred to the distinction between acrylate monomer, acrylate oligomer and pre-polymer. The IR spectra of blanket cross sections by IR imaging system were statistically analyzed using PCA. The IR spectra were classified into six particular principal components (PC). Figure 7 shows six PC spectra obtained by PCA. PC1 has the highest contribution in the IR imaging. In this case, PC1 depended on the blanket rubber. PC2 depended on the reinforcement cloth. It was confirmed that PC1 and PC2 image contrasts showed the blanket rubber and the reinforcement cloth, respectively. PC3 depended on the monomer because the characteristic peaks of PC3 corresponded with the IR peaks of acrylate monomer in Fig.6. Similarly,

PC4, PC5 and PC6 depended on the acrylate oligomer, pre-polymer and photo initiator, respectively. Because the acrylate monomer and acrylate oligomer used were liquid at the room temperature, the distribution of each acrylate into blankets was also estimated by single frequency images at 1735cm^{-1} (C=O stretching vibration) on the cross sections of blanket. As a result, the image contrasts of PC3 and PC4 were considerably corresponded with the distribution of acrylate monomer and acrylate oligomer respectively into blanket rubber.

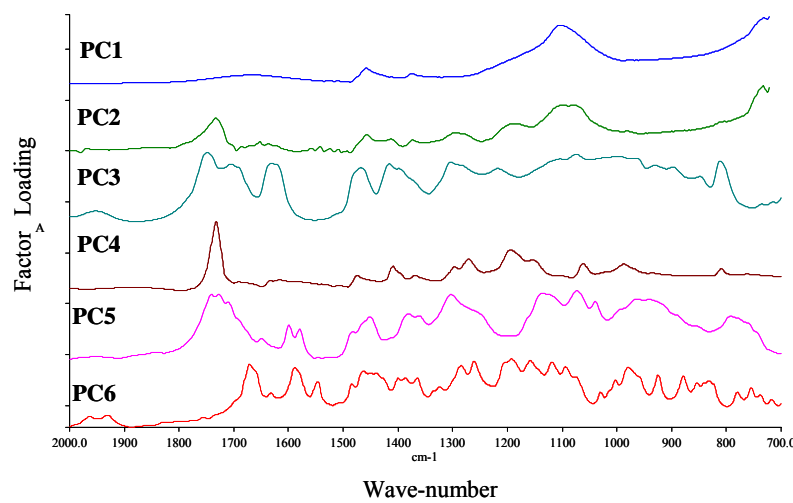


Figure 7 Six PC spectra (2000 to 700cm^{-1}) obtained by PCA

Figure 8 shows image contrasts of PC3, PC4, PC5 and PC6 which characterized acrylate monomer, acrylate oligomer, pre-polymer and photo initiator respectively. Each cross section sample was measured by the IR imaging system several hours after dropping on the blanket. The penetration rate of vehicle into the blanket was in order of acrylate monomer > acrylate oligomer > pre-polymer. In addition, the photo initiator transferred with monomer acrylate in the blanket.

In consequence of the penetration of each component, the reason why the penetration rate of acrylate-A was same as that of UV curable ink (Figure4 and Figure5) would be that the single frequency maps at 1735cm^{-1} indicated the penetration of acrylate monomer.

Figure 9 shows the relationship between the penetration depth and time after UV curable ink vehicle dropping. The acrylate monomer reached the boundary between blanket rubber and the reinforcement cloth first. Next, the acrylate

oligomer came to the boundary between the blanket rubber and the reinforcement cloth. However, pre-polymer arrived only at the middle of the blanket rubber 48 hours later after ink vehicle dropping. As well as the result in Fig.8, it was confirmed that the photo initiator penetrated with acrylate monomer in the blanket. This was because the photo initiator, having low molecular weight, could dissolve well in the acrylate monomer. It was suggested that UV curing property of ink on the new blanket would be different from that on the old blanket due to the penetration of acrylates and photo initiator into the blanket. Consequently, the penetration rate of each component in UV curable ink vehicle into the printing blanket could be evaluated from PCA data of IR imaging on cross sections of blanket for the first time.

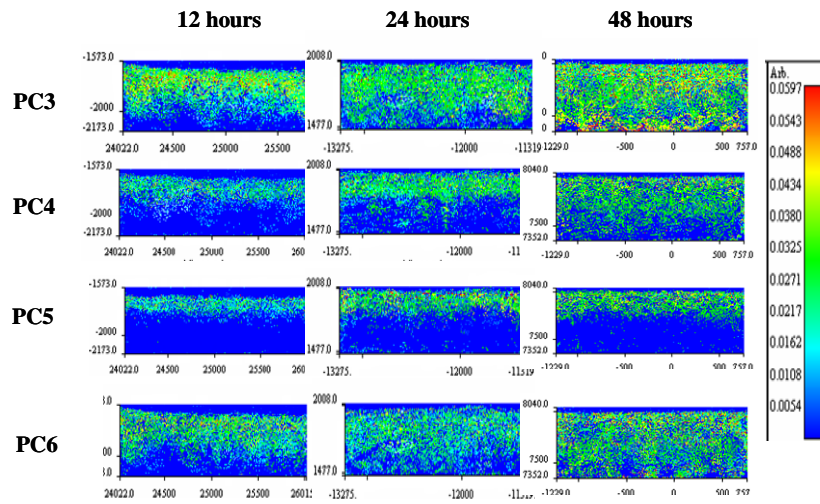


Figure 8 Image contrasts of PC3, PC4, PC5 and PC6 several hours after UV curable ink vehicle dropping

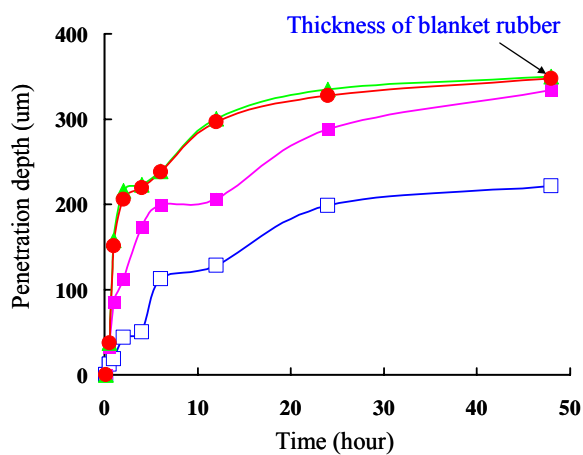


Figure 9 Relationship between penetration depth and time after UV curable ink vehicle dropping

▲:acrylate monomer, ■:acrylate oligomer, □: pre-polymer, ●:photo initiator

Conclusions

The penetration of UV curable ink vehicle into the printing blanket could be evaluated using IR imaging system. The distribution of acrylate into blanket rubber could be observed by the single frequency map at 1735cm^{-1} (C=O stretching vibration that depended on acrylate).

In addition, the penetration rate of each component in UV curable ink vehicle into printing blanket could be evaluated from PCA data of IR imaging on cross sections of blanket for the first time. As a result, acrylate monomer penetrated fastest, followed by acrylate oligomer, and pre-polymer penetrated very slowly. Moreover, acrylate monomer and acrylate oligomer could reach the boundary between rubber and reinforcement cloth, but pre-polymer could not penetrate as far as the middle of blanket rubber in 48 hours. In addition, it was also found that the photo initiator transferred together with monomer acrylate in the blanket.

Literature Cited

- Elliott, G. N., Worgan, H., Draper J., Scullion J., Broadhurst D.
2007 "Soil differentiation using fingerprint Fourier transform infrared spectroscopy, chemometrics and genetic algorithm-based feature selection", *Soil Biol. Biochem.*, vol.39, no.11, pp.2888-2896
- Green, A. A., Berman, M., Switzer, P., Craig, M. D.
1998 "A transformation for ordering multispectral data in terms of image quality with implications for noise removal", *Ieee Trans. On Geosci. & Remote Sci.*, vol.26, no.1, pp.65-74
- Lee, J. B., Woodyatt, S., Berman, M.,
1990 "Enhancement of high spectral resolution remote-sensing data by a noise-adjusted principal components transform", *Ieee Trans. On Geosci. & Remote Sci.*, vol.28, no.3, pp.295-304
- Marengo, E., Liparota M. C., Robotti, E., Bobb, M., Gennaro M. C.
2005 "Monitoring of pigmented surfaces in accelerated ageing process by ATR-FT-IR spectroscopy and multivariate control charts", *Talanta*, vol.66, no.5, pp.1158-1167
- Ozaki, Y., Bousfield, D.W. and Shala, S. M.
2007 "Characterization of Penetration of Solvents into Press Blankets by Confocal Laser Scanning Microscope", *TAGA J.*, Vol.3, pp.119-127
- Pereira, R. C. C., Skrobot V. L., Fortes, I. C. P., Pasa V. M. D.
2006 "Determination of Gasoline Adulteration by Principal Components Analysis-Linear Discriminant Analysis Applied to FTIR Spectra", *Energy & Fuels*, vol.20, no.3, pp.1097-1102
- Stowe, R.W.
2004 "UV as the Energy Source for Industrial Processing of Coatings, Inks, and Adhesives", *TAGA proceedings*, pp.89-104
- Sun, L., Sodhi, R. N. S., Farnood, R., Reeve D.W.
2004 "Analysis of ink/coating penetration on paper surfaces by time of flight secondary ion mass spectrometry (TOF-SIMS) in conjunction with principal component analysis (PCA)", *Proceeding of Int. Printing & Graphic Arts Conf.*, pp.95-101
- Vanden, E. X., Bertrand, P.
1997 "TOF-SIMS quantification of polystyrene spectra based on principal component analysis (PCA)", *Surf. Interface Anal.*, vol.25, no.11, pp.878-888